AJNR

Multidetector CT Angiography in Diagnosing Type I and Type IVA Spinal Vascular Malformations

P.H. Lai, M.J. Weng, K.W. Lee and H.B. Pan

This information is current as of June 30, 2025.

TECHNICAL NOTE

P.H. Lai
M.J. Weng
K.W. Lee
H.B. Pan

Multidetector CT Angiography in Diagnosing Type I and Type IVA Spinal Vascular Malformations

SUMMARY: Multidetector CT (MDCT) angiography is an imaging technique that can provide high-resolution and high-contrast images; however, published reports of MDCT angiography in the evaluation of spinal vascular malformations are limited. We present 2 cases in which MDCT angiography led to diagnosis of a type I (spinal dural arteriovenous fistula) in one and type IVA (perimedullary spinal cord simple arteriovenous fistula fed by a single arterial feeder) spinal vascular malformation, both confirmed by conventional angiography. MDCT angiography can localize the feeding vessel and the fistula, thus greatly reducing the amount of time required for conventional angiography.

Conventional angiography has been used as a primary imaging technique for the localization of the shunt of spinal dural arteriovenous fistulas (SDAVFs) and perimedullary spinal cord simple arteriovenous fistula (SCAVFs). Multidetector CT (MDCT) angiography is an imaging technique that can provide extended thin-section scanning range with high-resolution and high-contrast images.[1] There have been few preliminary reports in the diagnosis of SDAVFs by using MDCT angiography.[2,3] We present our preliminary experience in diagnosing type I and type IVA spinal vascular malformations in 2 cases with similar spinal MR imaging abnormalities, in which we used MDCT angiography.

Technique

CT Angiography

Two patients were referred for CT angiography (CTA) for evaluation of spinal vascular malformations, which were suspected on the basis of combined findings from spinal MR imaging and a radiculomyelopathy. Spinal CTA was performed with a 16-detector row helical scanner. The patients were placed in the supine position and were requested to hold their breath during the scanning period; the volume covered extended from the first thoracic spine down to the fifth sacrum region. The scan delay was set by an automatic bolus-tracking technique after the start of a bolus injection of 120 mL of nonionic contrast medium, followed by 30 mL of normal saline at a flow rate of 4 mL/s. A circular region of interest in the ascending aorta was measured 3 times per second. When the attenuation value reached a threshold of 100 HU in 3 consecutive sampling points, scanning began. The acquisition protocol was as follows: gantry speed per rotation, 0.5 seconds; collimation, 16×0.75 mm; table increment, 36 mm/s; 120 kVp; and 120 effective mAs. The total imaging time was 16 seconds. Sections were reconstructed with a 0.75-mm section thickness at 0.4-mm intervals; approximately 1200 reconstructed sections were obtained. Resultant voxel dimensions were nearly isotropic at $0.5 \times 0.5 \times 0.75$ mm.

Image Processing and Evaluation

Source images obtained with this MDCT angiographic technique were transferred to a workstation with manufacturer-provided software that allows generation of 2D multiplanar reformation (MPR), curved planar reformation (CPR), maximum intensity projection (MIP), and multiprojection volume reconstruction (MPVR) images. Volume-rendered images of the entire aorta were routinely generated. A 2-mm-thick transversely oriented thin-slab MIP image was produced, and this transverse slab was then sequentially stepped inferiorly on the template of the coronal image. In this fashion, the bilateral intercostal, lumbar, and iliac arteries were systematically visualized, which helped confirm their normal anatomic relationships and identify the spinal vascular malformation.

The level of the dural fistula was indirectly inferred by tracing an engorged medullary vein from the coronal venous plexus back to the level of a neural foramen. With use of the MPR and MPVR options, including oblique coronal and sagittal images, the imaged portions of the spine were systematically evaluated until the area of suspected fistula was identified in 3 planes. Finally, a CPR image was reconstructed. We used a cine-mode display, in which multiple original transverse sections, MIP, and MPR images can be observed by scrolling the images on the workstation. The workstation image processing and evaluation lasted approximately 20 minutes.

Results

Case 1

A 22-year-old man experienced numbness in the right lower extremity for 1 year and dull back pain recently for 2 weeks. Neurologic examination performed at the time of admission revealed slight motor weakness and slight hypesthesia in the right lower extremity. On MR imaging, multiple engorged intradural pial vessels, central hyperintense cord on T2-weighted imaging, and cord enhancement on postcontrast T1-weighted imaging were observed from the lower thoracic levels to the upper lumbar levels (Fig 1A). The reconstructed MPVR and CPR images showed a type A perimedullary SCAVF at the L2 spine level. It was fed solely from the anterior spinal artery that arises from the left T8 intercostal artery.

Many engorged outflow drainage veins also were noted (Fig 1B). Multiple selective catheter angiographic injections were performed, and only the left T8 intercostal artery injection showed a type A perimedullary SCAVF supplied by the mild enlarged anterior spinal artery (Fig 1C). Selective transarterial glue embolization of the fistula and proximal drainage veins was performed. The patient's neurologic condition was improved after embolization.

Fig 1. 22-year-old man with intradural perimedullary SCAVF.

A, Sagittal fast spin-echo T2-weighted MR image (left) and postgadolinium T1-weighted image (right) show multiple enlarged pial vessels along the surface of the cord. Intrinsic increased signal intensity centrally within the spinal cord (left) and abnormal enhanced cord (right) extend from the lower thoracic levels to the conus medullaris.

B, Oblique coronal multiprojection volume-reconstruction images with different plane projections show the fistula (left, *white arrowheads* [type A, perimedullary SCAVF]) at the lower L2 spine level supplied by the mildly enlarged anterior spinal artery (*large arrow*). Multiple engorged outflow veins draining both cephalic and caudal directions are also noted (*small arrows*). Curved planar reformation image (right bottom) delineates the aorta (Ao) and anterior spinal artery feeder from the left T8 intercostal artery.

C, Conventional angiography of the left T8 intercostal artery in early (left) and late (right) phases, anteroposterior view, shows similar depiction of Fig 1*B.* The posterior spinal artery (*black arrowheads*) was also injected via the left T8 intercostal artery but did not supply the fistula.

Case 2

A 55-year-old man experienced a 2-year history of progressive numbness and weakness in his lower extremities and urinary incontinence during the past year. Neurologic examination performed at the time of admission revealed motor weakness and hypesthesia in both lower extremities. MR imaging of the spine showed multiple engorged flow
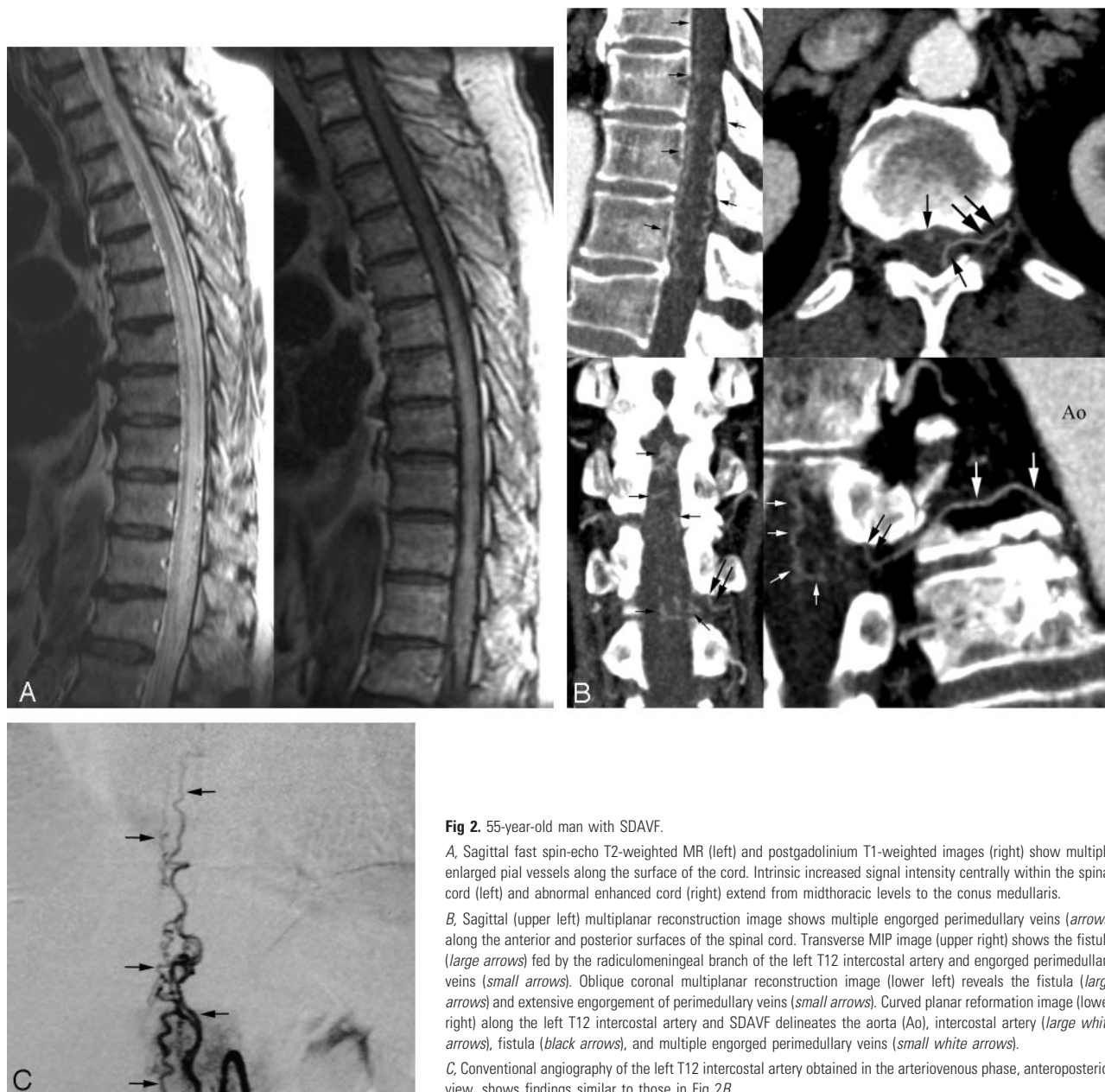
Fig 2. 55-year-old man with SDAVF.

A, Sagittal fast spin-echo T2-weighted MR (left) and postgadolinium T1-weighted images (right) show multiple enlarged pial vessels along the surface of the cord. Intrinsic increased signal intensity centrally within the spinal cord (left) and abnormal enhanced cord (right) extend from midthoracic levels to the conus medullaris.

B, Sagittal (upper left) multiplanar reconstruction image shows multiple engorged perimedullary veins (*arrows*) along the anterior and posterior surfaces of the spinal cord. Transverse MIP image (upper right) shows the fistula (*large arrows*) fed by the radiculomeningeal branch of the left T12 intercostal artery and engorged perimedullary veins (*small arrows*). Oblique coronal multiplanar reconstruction image (lower left) reveals the fistula (*large arrows*) and extensive engorgement of perimedullary veins (*small arrows*). Curved planar reformation image (lower right) along the left T12 intercostal artery and SDAVF delineates the aorta (Ao), intercostal artery (*large white arrows*), fistula (*black arrows*), and multiple engorged perimedullary veins (*small white arrows*).

C, Conventional angiography of the left T12 intercostal artery obtained in the arteriovenous phase, anteroposterior view, shows findings similar to those in Fig 2*B*.

void pial vessels along the surface of the cord, central hyperintense cord signal intensity on T2-weighted imaging, and cord enhancement on postcontrast T1-weighted imaging from the midthoracic levels to the upper lumbar levels (Fig 2*A*). The reconstructed MIP, MPR, and CPR images showed a SDAVF fed by the radiculomeningeal branch of the left T12 intercostal artery (Fig 2*B*) and confirmed at catheter spinal angiography (Fig 2*C*). The patient's neurologic condition was improved after surgical coagulation of the fistula and a proximal portion of the draining medullary vein.

Discussion

Spinal vascular malformations represent a heterogeneous group of vascular anomalies. These lesions have been categorized into 4 types in the commonly accepted classification scheme of Anson and Spetzler[4]: type I, SDAVFs between a dural branch of the spinal ramus of a radicular artery and an intradural medullary vein; type II, intramedullary glomus malformations; type III, extensive juvenile malformations, often extending to involve surrounding paraspinous tissues; and type IV, arteriovenous fistulas (AVFs) between an intradural extramedullary artery and a dilated perimedullary vein, commonly called "perimedullary spinal cord AVFs " (SCAVFs).

The most common of the 4 types of vascular malformation is the SDAVF, which is considered to be an acquired lesion.[4] SDAVF consists of a vascular shunt that is located in the dura along the spinal canal near the neural foramen region. The arterial supply commonly arises from a dural branch of the radicular artery, with venous drainage to the engorged perimedullary veins (coronal venous plexus).[5-7] SDAVF is most frequently located in the thoracic or lumbar levels, and >90% of the spinal dural AVFs are located between T1 and S3.[6,7] Although perimedullary SCAVFs are thought to be rare, some recent reports have suggested that these lesions are more common than previously indicated in the literature.[8,9] They are

most commonly observed in the conus medullaris or cauda equina, although cervical and thoracic perimedullary SCAVFs have also been reported.[8,9] Perimedullary SCAVFs have been further classified into 3 subtypes: simple fistulas fed by a single arterial branch (type A), intermediate-sized fistulas (type B), and giant multipediculated fistulas (type C).[4]

Findings of a SDAVF at conventional spin-echo MR imaging may include central hyperintensity on T2-weighted images within the lower spinal cord and conus medullaris, gadolinium enhancement within the cord, and multiple vascular flow voids along the surface of the spinal cord;[5-7] however, these findings are of minimal assistance in the characterization and localization of a malformation.

Perimedullary SCAVFs and SDAVFs might have fairly similar MR imaging findings as in our 2 cases if there is not a distinction made between an enlarged anterior spinal artery feeding the fistula (type IV) and the dural fistula having the shunt near the root sleeve region (type I).

Spinal MR angiography (MRA) techniques[10-14] have been well studied for increasing the sensitivity and specificity of suspected SDAVFs. In an early study, Bowen et al[10] identified the dominant vein and corresponding fistula level on an 11-minute standard 3D contrast-enhanced (CE) MRA in 67% (6/9) of the reported cases. In a later study, accurate prediction of Saraf-Lavi et al[11] of the correct fistula level increased from 15% for MR imaging alone to 50% for the combined study (MR imaging and standard 3D CE MRA), and the correct level ±1 was predicted in 73% for the combined study. More recently, auto-triggered elliptical ordered fast 3D CE MRA technique combined with a rapid bolus injection and a robust timing mechanism is a technical advance in spinal MRA for the evaluation of SDAVFs. The fast 3D method (scan time, <2 minutes) may be advantageous because it can display the arteriovenous shunt, which is not typically seen with the standard 3D method because of diffuse epidural enhancement.

The arteriovenous shunt was detected in 2 of 3 cases of SDAVF by Binkert et al[12] and in 8 of 9 cases by Farb et al.[13] In the latter study, the number of 3D MRA examinations required to confidently identify the site before digital subtraction angiography was as follows: 1 MRA in 4 patients, 2 MRAs in 4 patients, and 3 MRAs in 1 patient. Luetmer et al[14] obtained 2 overlapping acquisitions to prevent the repeated difficulty of fistulas located outside the image volume. One fistula occurred outside the imaging volume in the sacrum. Preangiographic MRA localization of the fistula was associated with a dramatic reduction of >50% in fluoroscopy time and volume of contrast agent.

To obtain substantial arterial visualization on CTA, one must perform data acquisition while the bolus of intravenously administered contrast medium is filling the vessels to be imaged. MDCT systems can use 4 rows of detectors and can provide similar image quality at a speed gain of 3–6 times greater than that of single-detector CT.[1] This results in larger anatomic coverage. Moreover, MDCT scanning can produce higher spatial resolution than single-detector CT. With these capabilities, the artery of Adamkiewicz could often be depicted (68%–90%) on CTA with a 4-detector row helical scanner.[15,16] In the study by Yoshioka et al,[17] the artery of Adamkiewicz was detected more often by 4-detector row CT than by

MRA in patients with thoracoabdominal aortic aneurysm (80% versus 66.7%).

Sixteen-detector row spinal CTA[3] provides a very short scanning time and more scan length coverage (∼55 cm), and higher spatial resolution (0.5 × 0.5 × 0.75 mm) compared with 3D CE MRA (36 cm; 1.0 × 1.0 × 1.2 mm)[13] in diagnosing SDAVFs. Farb et al[13] reported that repeated double/triple MRA was required to search for the SDAVF in another region in more than half of the patients.[13] In contrast, with the MDCT method, the added imaging volume was easily done in the craniocaudal direction, with an additional several seconds of examination. Another advantage of CTA is to allow observation of enhanced vessels among the bony spine structures. Even if MRA demonstrates abnormal vessels sufficiently, localization of the fistula in relation to the spinal cord and bony structures is not easy because flow-related artifacts and the signal intensity from the spinal cord, CSF, and bony structures are usually suppressed and hardly recognized on MRA.

MDCT angiography is feasible and is an alternative technique in diagnosing SDAVF.[2,3] Bertrand et al[2] reported 1 case of left T11 SDAVF on CTA with a 16-detector row helical scanner and confirmed by conventional angiography. Lai et al[3] reported a small series of 8 cases of SDAVFs, 7 at the thoracic level and 1 at the sacral level by using 16-detector row CT. MDCT angiography was good at detecting the fistula, feeding artery, and draining veins of the SDAVFs and correlated well with conventional angiography. One patient with an additional feeding artery was not identified with CTA. In the newly developed 64-detector systems, the primary benefits of the higher spatial and temporal resolutions and isotropic volume data compared with 16-detector CT systems will be anticipated.

The search for a SDAVF with conventional angiography is often tedious and requires selective injections into multiple bilateral thoracic intercostal, lumbar, and sacral arteries. If no fistula is found, then cervical and intracranial regions are sequentially explored. An exhaustive search for an SDAVF may include as many as 40 selective injections.[18] The ability to predict the arterial feeder noninvasively by spinal CTA can potentially expedite the subsequent invasive catheter angiography examination by directing the angiographer to certain spinal levels initially. When results of preangiographic CTA suggested the location of the SDAVF, selective manual injections were performed at this level first. If the fistula was identified, the contralateral segmental artery and the segmental arteries 1 level above and 1 level below the fistula were studied to ensure complete evaluation of the fistula and the adjacent vasculature. The commonly lengthy conventional angiography sessions could be shortened by more than half of the time.[14]

The disadvantages of spinal CTA are the use of ionizing radiation as well as intravenous contrast agent and its inherent risks. We opted to evaluate the field of view from the thoracic spine to the sacrum to include >90% of SDAVFs, not including the intracranial and cervical spine regions, for minimizing the radiation dose delivered to the patients. We assessed the effective dose calculations by application of the CT dosimetry spreadsheet of the British Imaging Performance Assessment of CT group.[19] The average effective dose for our spinal CTA was 9.1 mSv.

The success of spinal CTA of our 2 cases in showing the

SDAVF and type A perimedullary SCAVF is more easily obtained because of a simpler angioarchitecture comprising 1 single arterial feeder and its fistula. MPR, CPR, and MPVR images in regions of interest may improve identification of feeding arteries and fistulas. Review of the source images can also help in identifying the vessels in question. The multiple arterial feeders of spinal vascular malformations possibly represent a more diagnostic challenge in MDCT angiography, and a large series of patients are needed to test in the future.

In common with 3D CE MRA, the temporal resolution of 16-detector-row CTA is not sufficient to distinguish arterial feeders from draining veins in spinal AVFs, compared with conventional angiography. Conventional angiography is still mandatory before embolization to allow extensive characterization of the spinal AVFs and identification of macroscopic additional feeding arteries and to determine whether an anterior spinal artery arises from the same pedicle that supplies the dural fistula. If the same radicular artery supplies the SDAVF and anterior spinal artery, it may indicate a contraindication for endovascular therapy.

In conclusion, MDCT angiography may diagnose type I and type IVA spinal vascular malformations in 2 cases of similar abnormalities on MR imaging. This technique can localize the supplied vessel and fistula and thus greatly reduce the amount of time required for conventional angiography; however, further large studies are required to assess the sensitivity and specificity of MDCT angiography versus MRA in the diagnosis and pretherapeutic evaluation of perimedullary SCAVFs and SDAVFs.

References

1. Rubin GD, Shiau MC, Schmidt AJ. **Computed tomographic angiography: historical perspective and new state-of-the-art using multi detector-row helical computed tomography.** *J Comput Assist Tomogr* 1999;23(suppl 1):S83–90
2. Bertrand D, Douvrin F, Gerardin E, et al. **Diagnosis of spinal dural arteriovenous fistula with multidetector row computed tomography: a case report.** *Neuroradiology* 2004;46:851–54
3. Lai PH, Pan HB, Yang CF, et al. **Multi-detector row computed tomography angiography in diagnosing spinal dural arteriovenous fistula: initial experience.** *Stroke* 2005;36:1562–64
4. Anson JA, Spetzler RF. **Classification of spinal arteriovenous malformations and implications for treatment.** *Barrow Neurol Inst Quarterly* 1992;8:2–8
5. Gilbertson JR, Miller GM, Goldman MS, et al. **Spinal dural arteriovenous fistulas: MR and myelographic findings.** *AJNR Am J Neuroradiol* 1995;16:2049–57
6. Atkinson JLD, Miller GM, Krauss WE, et al. **Clinical and radiographic features of dural arteriovenous fistulas; a treatable cause of myelopathy.** *Mayo Clin Proc* 2001;76:1120–30
7. Van Dijk JM, TerBrugge KG, Willinsky RA, et al. **Multidisciplinary management of spinal dural arteriovenous fistulas: clinical presentation and long-term follow-up in 49 cases.** *Stroke* 2002;33:1578–83
8. Mourier KL, Gobin YP, George B, et al. **Intradural perimedullary arteriovenous fistulae: results of surgical and endovascular treatment in a series of 35 cases.** *Neurosurgery* 1993;32:885–91
9. Barrow DL, Colohan AR, Dawson R. **Intradural perimedullary arteriovenous fistulas.** *J Neurosurg* 1994;81:221–29
10. Bowen BC, Fraser K, Kochan JP, et al. **Spinal dural arteriovenous fistulas: evaluation with magnetic resonance angiography.** *AJNR Am J Neuroradiol* 1995;16:2029–43
11. Saraf-Lavi E, Bowen BC, Quencer RM, et al. **Detection of spinal dural arteriovenous fistula with MR imaging and angiography: sensitivity, specificity, and prediction of vertebral level.** *AJNR Am J Neuroradiol* 2002;23:858–67
12. Binkert CA, Kollias SS, Valavanis A. **Spinal cord vascular disease: characterization with fast three-dimensional contrast-enhanced MR angiography.** *AJNR Am J Neuroradiol* 1999;20:1785–93
13. Farb RI, Kim JK, Willinsky RA, et al. **Spinal dural arteriovenous fistula localization with a technique of first-pass gadolinium-enhanced MR angiography: initial experience.** *Radiology* 2002;222:843–50
14. Luetmer PH, Lane JI, Gilbertson JR, et al. **Preangiographic evaluation of spinal dural arteriovenous fistulas with elliptic centric contrast-enhanced MR angiography and effect on radiation dose and volume of iodinated contrast material.** *AJNR Am J Neuroradiol* 2005;26:711–18
15. Takase K, Sawamura Y, Igarashi K, et al. **Demonstration of the artery of Adamkiewicz at multi-detector row helical CT.** *Radiology* 2002;223:39–45
16. Kudo K, Terae S, Asano T, et al. **Anterior spinal artery of Adamkiewicz detected by using multi-detector row.** *AJNR Am J Neuroradiol* 2003;24:13–17
17. Yoshioka K, Niinuma H, Ohira A, et al. **MR angiography and CT angiography of the artery of Adamkiewicz: noninvasive preoperative assessment of thoracoabdominal aortic aneurysm.** *RadioGraphics* 2003;23:1215–25
18. Willinsky RA, Lasjaunias P, TerBrugge KG. **Angiography in the investigation of spinal dural arteriovenous fistula: a protocol with application of the venous phase.** *Neuroradiology* 1990;32:114–16
19. Jones DG, Shrimpton PC. **Survey of CT practice in the UK: normalised organ doses for X-ray computed tomography calculated using Monte Carlo techniques.** *National Radiological Protection Board* Harwell UK. 1991. Available at: http://www.impactscan.org/ctdosimetry.htm. Accessed May 2004